Journal of Inflammation Research

Dovepress
Taylor & Francis Group

Open Access Full Text Article

ORIGINAL RESEARCH

Volatile Oil From *Acorus Gramineus* Rhizoma Synergizes with Crebanine to Alleviate Oxidative Stress and Endoplasmic Reticulum Stress in Myocardial Ischemia-Reperfusion Injury by Suppressing GRP78-PERK/ATF6-CHOP and MAPK-NF-κB-TNF-α Signaling Pathways

Lichun Zha[1,2,*], Lili Cui[1,3,*], Jiahua Mei[1,4,*], Juan Pu[1,3], Jiaxu Hao[1,4], Xiao Fan[1,4], Hongyuan Wang[1,3], Heng Fang[1], Yunshu Ma[1,3,4]

[1]School of Chinese Materia Medica of Yunnan University of Traditional Chinese Medicine, Kunming, Yunnan, 650500, People's Republic of China; [2]Zhaotong Hospital of Traditional Chinese Medicine, Zhaotong, Yunnan, 657000, People's Republic of China; [3]The Key Laboratory of External Drug Delivery System and Preparation Technology in University of Yunnan Province, Kunming, Yunnan, 650500, People's Republic of China; [4]Yunnan Key Laboratory of Dai and Yi Medicines, Kunming, Yunnan, 650500, People's Republic of China

*These authors contributed equally to this work

Correspondence: Yunshu Ma, Yunnan University of Traditional Chinese Medicine, 1076 Yuhua Road, Kunming, Yunnan, 650500, People's Republic of China, Email yunshuma2@126.com

Purpose: To investigate the synergistic protective effects and underlying mechanisms of combining *Acorus gramineus* rhizoma volatile oil (VOA), known for its "Cardiotropic-channel-directing" properties, with Crebanine (Cre) in MIRI.

Patients and Methods: An MIRI model was established in Sprague-Dawley rats to evaluate the synergistic cardioprotective effects of VOA combined with Cre. Myocardial injury was assessed by measuring the infarct size, apoptotic cardiomyocytes, myocardial injury biomarkers, and histopathological changes. Proinflammatory mediators and oxidative stress markers and results of Western blotting were analyzed to determine the underlying cardioprotective mechanisms of Cre and VOA. In addition, metabolomic analysis was conducted to identify alterations in relevant metabolic pathways.

Results: Cre and VOA alleviated MIRI in rats by reducing infarct size, lowering the levels of myocardial injury biomarkers (Lactate dehydrogenase (LDH), cardiac troponin I (cTnI), creatine kinase (CK), and creatine kinase-myocardial band (CK-MB)), and ameliorating histopathological damage. Mechanistically, Cre and VOA attenuated oxidative stress by enhancing the activity of the antioxidant enzyme superoxide dismutase (SOD) and suppressing the expression of the oxidative stress marker malondialdehyde (MDA). In addition, they downregulated proinflammatory cytokines (interleukin-6 (IL-6) and interleukin-1β (IL-1β)) by inhibiting the MAPK/NF-κB/TNF-α signaling pathway. They mitigated endoplasmic reticulum (ER) stress and apoptosis by modulating the GRP78-PERK/ATF6-CHOP pathway. Metabolomic analysis identified 13 potential biomarkers, and glutamic, pantothenic, and oleic acids were the key metabolites. The glycine, serine, and threonine metabolism pathway, glutathione metabolism, the pentose phosphate pathway, and the biosynthesis of unsaturated fatty acids were the most relevant metabolic pathways involved in the cardioprotective effects of Cre and VOA.

Conclusion: Cre and VOA may alleviate MIRI by modulating energy metabolism and suppressing apoptosis and inflammatory responses triggered by oxidative and ER stress. This effect is mediated by GRP78-PERK/ATF6-CHOP and MAPK-NF-κB-TNF-α signaling pathways. Moreover, the volatile oil of *Acorus tatarinowii* significantly enhanced the cardioprotective effects of Cre against ischemia-reperfusion injury.

Keywords: apoptosis, inflammation, myocardial ischemia, cardioprotective, energy metabolism

Received: 10 April 2025
Accepted: 27 August 2025
Published: 17 September 2025

Graphical Abstract

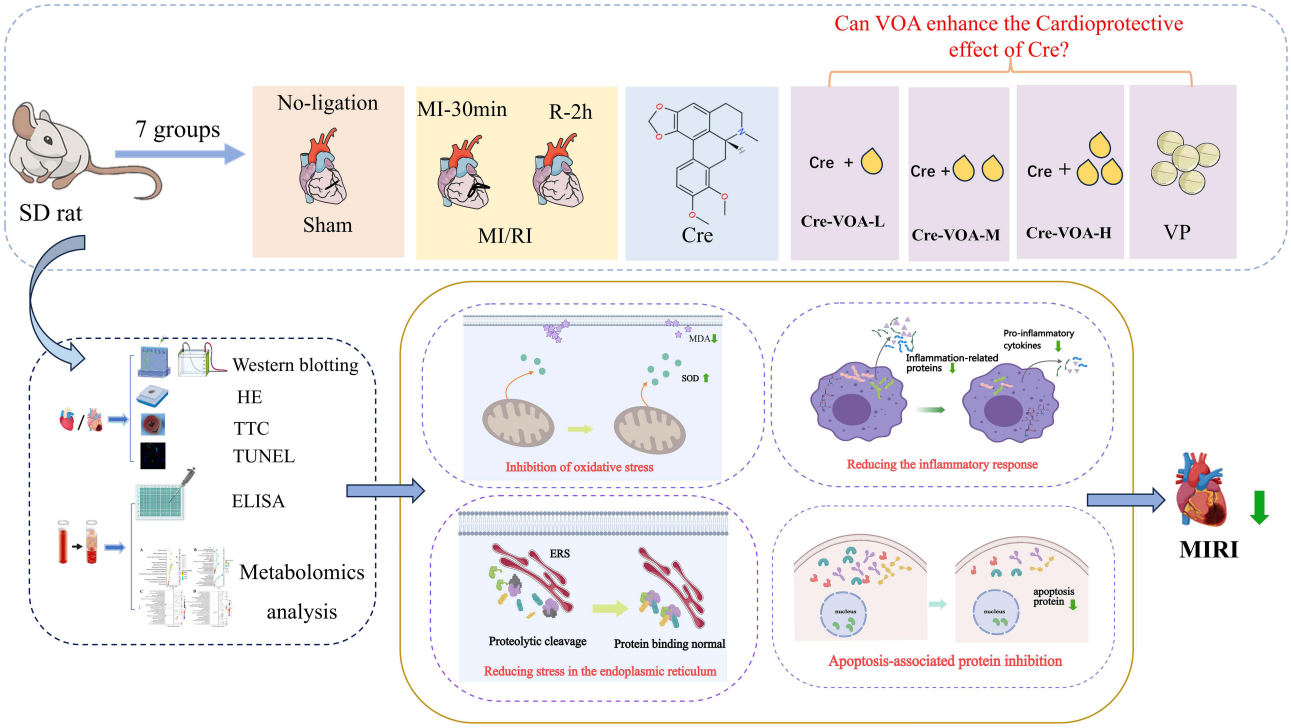

Introduction

Globally, ischemic heart disease is the primary cause of cardiovascular diseases and mortality.[1] Myocardial ischemia-reperfusion (MI/R) is an unavoidable process when treating myocardial ischemia (MI). However, reperfusion can lead to more severe myocardial injury, sometimes exceeding its beneficial effects. Myocardial ischemia-reperfusion injury (MIRI) is triggered by various factors, including inflammation, calcium overload, cell apoptosis, oxidative stress, and endoplasmic reticulum stress (ERS). Safe and effective drugs for alleviating MIRI are currently lacking.[2] Given the complex pathophysiology of MIRI, developing multidimensional therapeutic strategies remains a valuable area of investigation.

Oxidative stress plays a crucial role in MIRI. Excessive production of reactive oxygen species (ROS) occurs during reperfusion following ischemia. When ROS levels exceed the cellular antioxidant capacity, redox homeostasis is disrupted, leading to oxidative stress. In addition, elevated ROS levels can impair the transmembrane potential of the mitochondrial membrane, reducing intracellular adenosine triphosphate (ATP) synthesis and ultimately leading to oxidative cellular damage.[3,4] Growing evidence has shown that oxidative stress activates apoptotic signaling pathways and triggers acute inflammatory responses, further exacerbating myocardial injury.[5,6] The endoplasmic reticulum (ER) is a cellular organelle that plays a key role in protein synthesis. Ischemia and hypoxia can lead to abnormal protein folding and accumulation within cells, thereby triggering ERS.[7] ERS involves various physiological and pathological processes, including inflammation, cell apoptosis, energy metabolism, and oxidative stress.[8] Excessive ERS can induce apoptosis and synergistically interact with oxidative stress to form a vicious cycle of cellular damage. Inhibiting ERS effectively reduces myocardial damage caused by ischemia-reperfusion (IR).[9] Furthermore, inflammatory response is a critical component of MIRI. During MIRI, high numbers of neutrophils are drawn to the tissue or caused to adhere to the myocardial vascular endothelium due to the damaged membrane structures of the myocardial endothelial tissues. This induces the production of proinflammatory cytokines and activates an inflammatory reaction, leading to MI.[10] Apoptosis is a significant physiological and pathological process in IR, which leads to cell necrosis and myocardial tissue damage.

Therefore, attenuating myocardial injury by suppressing oxidative stress and ERS, which reduces inflammation and apoptosis, may be a feasible and effective therapeutic approach.

Traditional Chinese medicine (TCM) extracts, monomers, and their compound formulations, validated through historical applications, have gained widespread recognition in the treatment and prevention of cardiovascular disorders.[11–15] Compared to single-channel drugs, these formulations have a better side effect profile and can exert their effects through multiple channels and pathways, offering unique advantages in the prevention and treatment of cardiovascular diseases. The combination of TCM and Western medicine demonstrates stronger efficacy than Western medicine alone.[16–18] Thus, developing novel natural drugs with cardiovascular therapeutic effects holds significant potential.

Cre is an aporphine-type alkaloid isolated from *Stephanina yunnanensis* H. S. Lo, a species of the Menispermaceae family Stephania, along with several other plants of the same genus. Cre exhibits significant cardiovascular activity. Studies have shown that Cre can modulate the $I_{Ca\text{-}L}$, I_{K1}, and I_{Na} ion channels and reduce MIRI in rat models by regulating the expression of oxidative stress-related enzymes, thereby decreasing the myocardial infarct area and delaying the onset of arrhythmias induced by MI/R.[19] Therefore, Cre may exert its anti-arrhythmic and cardioprotective effects through multiple targets and pathways. However, the potential mechanisms by which Cre protects against MIRI remain largely unexplored and warrant further investigation.

Acorus gramineus rhizoma is derived from the dried rhizome of *Acorus tatarinowii*, a plant in the family Araceae.[19,20] The primary active components of *Acorus gramineus* rhizoma volatile oil (VOA), α-asarone and β-asarone, account for 95% of the volatile oil content.[19,21,22] The volatile oil from *Acorus* and β-asarone can alleviate MIRI by inhibiting oxidative stress and inflammation.[23,24] VOA and β-asarone exert anti-myocardial ischemia effects by reducing levels of endothelin, norepinephrine, and calcitonin gene-related peptide while enhancing nitric oxide production in rat models. In addition, the treatment reduces malondialdehyde (MDA) and creatine kinase levels and increases serum superoxide dismutase (SOD) activity. β-asarone also alleviates MIRI by suppressing inflammation and pyroptosis mediated by the NOD-like receptor family pyrin domain-containing 3 inflammasome.[23] However, current research on the protective effects of VOA against MIRI remains limited, and further studies are required to elucidate its underlying mechanisms. According to TCM theory, *Acorus gramineus* rhizoma belongs to the heart meridian. Meridian tropism is the ability of certain drugs to direct other medications to the area of disease. Previous pharmacokinetic studies by our research group revealed that, compared to Cre flexible liposome gels without VOA, the flexible liposome gels containing VOA significantly increased Cre absorption and distribution in the myocardial tissue in rats. Further research is required to determine whether oral administration of VOA can enhance the cardiac protective effects of Cre by increasing its distribution within the myocardial tissue.

The potential mechanisms by which Cre and VOA protect against MIRI remain largely unexplored. Based on previous literature and our preliminary findings, we aimed to investigate the synergistic effects of VOA—known for its "guiding drug into the heart" property—with Cre in MIRI. Specifically, we explored whether VOA enhances the cardioprotective effects of Cre and examined the underlying regulatory mechanisms from the perspectives of anti-oxidative stress and anti-ERS responses.

Materials and Methods

Drug Preparation

Cre was dissolved in 1% citric acid and adjusted to a pH of 5–6 with a saturated NaOH solution. The VOA was dissolved in 5% Tween 80. Then, Cre and VOA were diluted using purified water to achieve the specified concentration.

Animals

Male Sprague-Dawley rats weighing 200 ± 10 g were procured from the SPF (Beijing) Biotechnology Co., Ltd. (Animal Conformity Certificate No.: SYXK(Dian)K2017-0005). The rats were kept under conditions of constant temperature (24 ± 1°C), humidity (60 ± 5%), and 12-h light/dark cycles (8AM to 8PM).

Experimental Instruments

The instruments used included a Spectra max pLμs384 enzyme labeling instrument (MoLecuLar devices, America), BL-420 Biological Function Experiment System (Chengdu Taimeng Biotechnology Co., Ltd)., Electrophoresis Power Supply and Electrophoresis instrument (Bio-Rad, USA), a multifunctional molecular gel imaging system (Analytik Jena AG, Germany), mass spectrometer (Thermo Fisher Scientific Inc, USA), orthogonal fluorescence microscope (Nikon, Japan), imaging system (Nikon, Japan), ultra-high-pressure liquid chromatography (UHPLC, Shimadzu, Japan), and vacuum centrifuge concentrator (Eppendorf, Germany).

Reagents and Antibodies

Cre (content determination by HPLC, purity ≥98%) and VOA (concentration of 0.84 g/mL) were produced by the Institute of Yunnan University of Traditional Chinese Medicine. Verapamil Hydrochloride Tablets (VP, 20210522) were provided by Tianjin Central Pharmaceuticals Co. (Tianjin, China). Tween 80 (20180718) was purchased from Sinopharm Chemical Reagent Co. The creatine kinase (CK) assay kit (MM-20460R2), the Cardiac Troponin I (cTnl) assay kit (MM-61550R2), the creatine kinase MB isoenzyme (CK-MB) assay kit (MM-0625R2), the SOD assay kit (MM-0386R2), the MDA assay kit (MM-0385R1), the lactate dehydrogenase (LDH) assay kit (MM-0873R2), the Interleukin-6 (IL-6) assay kit (MM-0190R1), the Interleukin-1β (IL-β) assay kit (MM-0047R2), and the Tumor Necrosis Factor-α (TNF-α) assay kit (MM-0180R2) were produced from the Jiangsu Enzyme Immunity Industry Co. (Jiangsu, China). The phosphate-buffered saline (PBS, G0002), 4′,6-diamidino-2-phenylindole (DAPI, G1012, a fluorescent dye), and the Terminal deoxynucleotidyl transferase dUTP Nick End Labeling (TUNEL) assay kit (G1501) were purchased from Servicebio. The highly efficient radioimmunoprecipitation assay (RIPA) tissue rapid lysate was purchased from Solarbio. The antibodies used in this study are listed in Table 1.

Establishment of Myocardial Ischemia-Reperfusion Injury Model

Ninety-eight Sprague-Dawley rats (weighing 180–220 g) were acclimated for 1 week and housed in a specific pathogen-free room at a controlled temperature of 25 ± 2°C under a 12-h light/dark cycle. The rats were randomly assigned to seven groups (n=14 per group): Sham, Model, VP, Cre, Cre-VOA-L, Cre-VOA-M, and Cre-VOA-H. The rats in the Model group were subjected to 30 min of myocardial ischemia followed by 2 h of reperfusion, as described below: Surgical anesthesia was induced by an abdominal injection of the anesthetic agent pentobarbital (30 mg/kg). The

Table 1 Antibody Information Sheet

Name	Lot Number	Manufacturer
GRP78/BIP Polyclonal Antibody	11587-1-AP	Proteintech
CHOP Polyclonal Antibody	15204-1-AP	Proteintech
Caspase-3 Polyclonal Antibody	19677-1-AP	Proteintech
Caspase-9 Polyclonal Antibody	10380-1-AP	Proteintech
Bax Polyclonal Antibody	505991-2-Ig	Proteintech
Bcl-2 Polyclonal Antibody	26593-1-AP	Proteintech
ATF-6 Polyclonal Antibody	24169-1-AP	Proteintech
PERK Polyclonal Antibody	24390-1-AP	Proteintech
p38 MAPK Polyclonal Antibody	14064-1-AP	Proteintech
Anti-phospho-PERK Polyclonal Antibody	bs-3330R	Bioss
Anti-phospho-p38 MAPK Polyclonal Antibody	bs-0636R	Bioss
Anti-phospho-NF-κB p56 Polyclonal Antibody	GOYK98596	Cell Signaling Technology
NF-κBp65	bs-0982R	Bioss
Phospho-NF-KB p65 Rabbit mAb	GOYK98596	Cell SignalingTechnology
GAPDH Rabbit Polyclonal Antibody	10494-1-AP	Proteintech
Anti-beta-Actin Polyclonal Antibody	bs-0061R	Bioss
HRP-conjugated Affinipure Goat Anti-Rabbit IgG (H+L)	SA00001-2	Proteintech

anesthetized rat was secured in a supine position on the operating board. Excess hair was shaved from the chest area using a shaving razor. A small incision was made in the left thoracic region, and the fascia was removed using forceps and scissors. A blunt dissection of the muscle tissue was performed to access the thoracic cavity. The intercostal space between the third and fourth ribs was retracted, and the pericardium was torn to expose the heart. The heart was extracted manually by pressing the rat's upper back. The left anterior descending coronary artery was ligated, after which the heart was reset, and the wound was sutured. Following 30 min of MI, the ligatures were released to allow reperfusion for 120 min. In the sham group, after open heart surgery, the rat heart was threaded without ligation, while all other steps were consistent with those in the model group. Successful modeling was confirmed by pale or dark purple discoloration of the left ventricular front wall in the rats, along with ST-segment elevation on the electrocardiogram. The ischemic myocardium gradually returned to a healthier red color after blood flow was restored. Rats in the VP group were orally administrated VP 10 mg/kg. Rats in the Cre group were orally administrated Cre 50 mg/kg. Rats in the Cre-VOA-L group were orally administrated Cre 50 mg/kg and VOA 25 mg/kg. Rats in the Cre-VOA-M group were orally administrated Cre 50 mg/kg and VOA 50 mg/kg. Rats in the Cre-VOA-H group were orally administrated Cre 50 mg/kg and VOA 100 mg/kg. Rats in the Sham and Model groups were given an equivalent amount of saline. The rats in each group were administered the medication as stated above once daily for 5 consecutive days before surgery. At the end of the procedures, the rats were sacrificed, and myocardial tissues and blood samples from the abdominal aorta were harvested.

Triphenyl Tetrazolium Chloride Staining

The myocardial tissue was harvested from the dead experimental animals, processed, and sectioned into slices 1–1.5 mm thick. The slices were subjected to staining with a 1% Triphenyl tetrazolium chloride (TTC) solution at 37°C for 20 min, fixed in 10% formaldehyde, and captured using a camera. The regions with MI appeared white on the resulting images, while areas unaffected by the infarction retained a red hue. Myocardial infarct area (%) = (infarcted area / total myocardial slice area) × 100%.

Hematoxylin-Eosin Staining

The left ventricular myocardial tissue was excised and fixed in 4% paraformaldehyde for 24 h. Subsequently, paraffin-embedded sections (4 μm) were stained sequentially with hematoxylin and eosin (H&E) for 5 min each and observed under a microscope.

TUNEL Staining

Rat hearts were fixed overnight at 4°C in paraformaldehyde, then embedded in paraffin and sectioned. After dehydration and deparaffinization, the tissue sections (5 μm) were digested with Proteinase K for 20 min at 37°C. Next, 50 μL of equilibration buffer was added to the tissue sections, ensuring complete coverage of the target area, and incubated at room temperature for 10 min. Subsequently, 57 μL of TdT incubation buffer was added, and the sections were incubated at 37°C for 1 h. Then, the sections were transferred to a staining jar containing PI solution or DAPI solution and incubated at room temperature for 8 min. Finally, the sections were mounted and examined under a microscope. TUNEL-positive cells in cardiac tissue were visualized, and the apoptotic rate was calculated using ImageJ software as follows: apoptotic rate = (TUNEL-positive cells/total cardiomyocytes) × 100%.

Enzyme-Linked Immunosorbent Assay Analysis

Blood samples were collected 2 h after reperfusion, and the serum was separated. Serum biochemical parameters, including CK, CK-MB, cTnI, LDH, MDA, SOD, and proinflammatory factors (IL-1β, TNF-α, and IL-6), were measured according to the instructions of the enzyme-linked immunosorbent assay (ELISA) kits.

Western Blotting

Using RIPA lysis buffer, total protein was extracted from the myocardial tissue of the Sham group, I/R group, and other drug-treated groups. The blood samples were centrifuged, followed by aspiration of the sera and quantification of the

protein concentration using the Bicinchoninic Acid assay kit. The proteins were separated via Sodium Dodecyl Sulfate–Polyacrylamide Gel Electrophoresis using gels with appropriate concentrations based on the molecular weight of the target proteins. The proteins were transferred to a polyvinylidene fluoride membrane after separation under constant voltage (100 V)/current (300 mA) conditions with ice bath cooling during the transfer process. Then, the membranes were blocked with 8% non-fat milk solution for 1 h to prevent non-specific binding. After blocking, the membrane was incubated overnight at 4°C or for 2 h at room temperature with primary antibodies (all 1:1000). The membrane was washed thrice with PBS and incubated with the appropriate secondary antibody at ambient temperature for 1 h to specifically bind to the primary antibody. Protein bands were visualized using a gel imaging system, and the intensity of the bands was correlated with the corresponding protein expression levels. Protein band intensities were quantified using ImageJ software. The data underwent dual normalization (internal reference correction followed by blank group normalization). Statistical comparisons and data visualization were performed using GraphPad Prism (version 8.0.1).

Metabolomics Analysis

Extraction of Metabolites

A 100 μL aliquot of the sample was mixed with 400 μL of prechilled acetonitrile-methanol solution (1:1 v/v) and homogenized through vigorous vortex mixing. Subsequent processing involved 1-h ultrasonic treatment under ice-cooled conditions. Following this, the solution underwent cryogenic preservation at −20°C for 60 min. Then, centrifugation was conducted at 4°C for 20 min (14,000 × g) to separate phases. The resulting supernatant was carefully collected and subjected to vacuum desiccation before Liquid Chromatography–Mass Spectrometry (LC-MS) examination.

LC-MS Data Acquisition

The LC-MS/MS analyses were conducted using a SHIMADZU-LC30 ultra-high-performance liquid chromatography (UHPLC) system; the chromatographic column used was the ACQUITY UPLC® HSS T3 (2.1×100 mm, 1.8 μm) column (Waters, Milford, MA, USA), coupled with QE Plus mass spectrometer (Thermo Scientific).The mobile phases were: A: 0.1% formic acid aqueous solution and B: acetonitrile. The gradient elution program was as follows: 0–2 min: B 0%; 2–6 min: B 0–48%; 6–10 min: B 48–100%; 10–12 min: B 100%; 12–12.1 min: B 100–0%; 12.1–15 min: B 0%. The MS signal acquisition was performed in positive and negative ion modes using electrospray ionization.

Metabolomic Data Analysis

The raw data files were analyzed using MS-DIAL and matched with HMDB, MassBank and other public databases and a locally built metabolite standard library in Baipu, to achieve relative quantitative and precise qualitative outcomes. To assess metabolite variations, multivariate statistical approaches, including principal component analysis (PCA) and orthogonal partial least squares-discriminant analysis (OPLS-DA), were implemented to derive variable significance through projection (VIP) scores. For individual metabolite comparisons between groups, univariate statistical evaluation using a *t*-test was performed to establish statistical significance levels (p-values) and quantify differential expression through fold-change (FC) measurements. Differential metabolites were identified based on the following criteria: VIP > 1, p-value < 0.05, and $|\log2\ FC| \geq 1.0$. The identified differential metabolites were used to perform cluster analyses with the R package. The Kyoto Encyclopedia of Genes and Genomes (KEGG) database was used to investigate the functions of these metabolites and their involvement in metabolic pathways.

To investigate altered biological pathways, KEGG enrichment analysis was performed on the differential metabolite data through the KEGG database. Pathway enrichment assessments employed Fisher's exact probability test with False Discovery Rate correction for multiple comparisons. Statistically significant pathways were identified using a threshold of $p<0.05$ following false discovery rate correction.

Statistical Analysis

Statistical analysis was performed using GraphPad Prism 8.0.1 with Ordinary one-way analysis of variance (ANOVA). Post-hoc tests were conducted following ANOVA using Dunnett's Test. All data are presented as the mean ± standard

deviation, with $p < 0.05$ considered the threshold for statistical significance (* $p < 0.05$, ** $p < 0.01$, *** $p < 0.001$; $^{\#}$ $p < 0.05$, $^{\#\#}$ $p < 0.01$, $^{\#\#\#}$ $p < 0.001$).

Results

Cre and VOA Attenuate MIRI

Myocardial infarct size is a common and important indicator of the extent of I/R injury. Statistical analysis of the TTC staining results (Figure 1A and B) revealed a 42.05% increase in the myocardial infarct size in the Model group compared with the Sham group. Pretreatment with various interventions reduced the infarct area significantly: 28.54%, 26.61%, 15.45%, 8.50%, and 7.91% in the Cre, Cre-VOA-L, Cre-VOA-M, Cre-VOA-H, and VP groups, respectively. H&E staining (Figure 1C) revealed pathological changes in the myocardial tissue across the groups. In the Model group, myocardial fibers appeared partially loosened, fragmented, and disorganized, accompanied by cellular disintegration and dissolution, indicating severe myocardial injury. Notably, some fiber loosening and breakage remained after drug pretreatment. However, the extent of myocardial pathological damage was notably alleviated in I/R rats. In addition, compared with the Model group, all treatment groups exhibited significantly decreased levels of myocardial injury biomarkers, including CK, CK-MB, cTnI, and LDH (Figure 1D–G). Moreover, compared to the Cre group, Cre-VOA-L, Cre-VOA-M, and Cre-VOA-H groups exhibited a downward trend in the aforementioned indicators, with significant differences observed particularly in the Cre-VOA-M and Cre-VOA-H groups.

Cre and VOA Reduce Myocardial Apoptosis Induced by MIRI

The anti-apoptotic effects of Cre and VOA were assessed using TUNEL staining and Western blot analysis. The TUNEL staining results indicated that the apoptotic rate in the Model group was 30.81%. Pretreatment with Cre and VOA effectively reduced the apoptotic rate, with values of 18.28%, 14.39%, 13.27%, 8.89%, and 7.70% in the Cre, Cre-VOA -L, Cre-VOA-M, Cre-VOA-H, and VP groups, respectively (Figure 2A and B). In addition, Western blot analysis of apoptosis-related proteins revealed that Cre and VOA pretreatment decreased the expression of the pro-apoptotic proteins

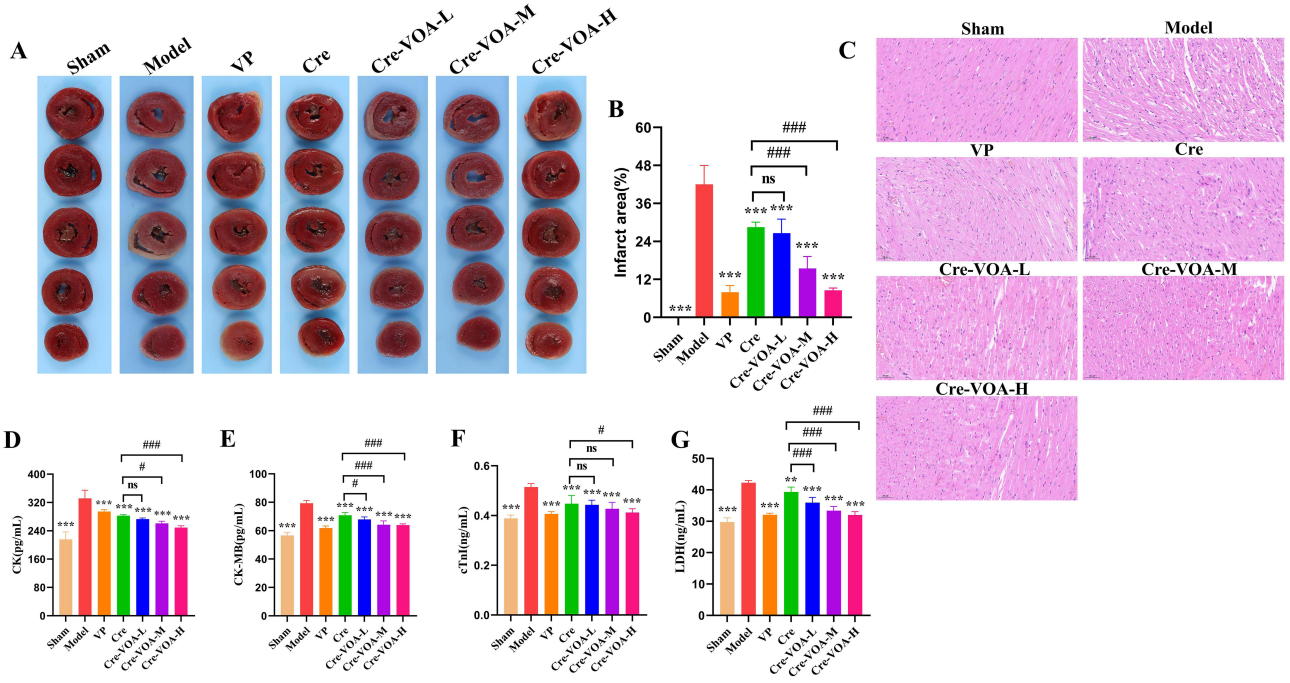

Figure 1 Cre and VOA reduce myocardial histopathological damage in MIRI Rats. (**A**) Myocardial tissue TTC staining: the red areas indicate non-damaged tissue, while the unstained white areas represent infarcted tissue. (**B**) infarct area is expressed as a percentage of the total area (n = 5). (**C**) HE staining depicting the extent of cardiac tissue injury in rats (×200, n = 6). (**D–G**) The levels of CK (**D**), CK-MB (BMC Ophthalmol), cTnI (**F**), and LDH (**G**) in the serum of Each group rats (n=6). *P < 0.05, **P < 0.01, ***P < 0.001 vs Model; #P < 0.05, ##P < 0.01, ###P < 0.001 vs Cre, ns indicates no significant difference.

https://doi.org/10.2147/JIR.S527105

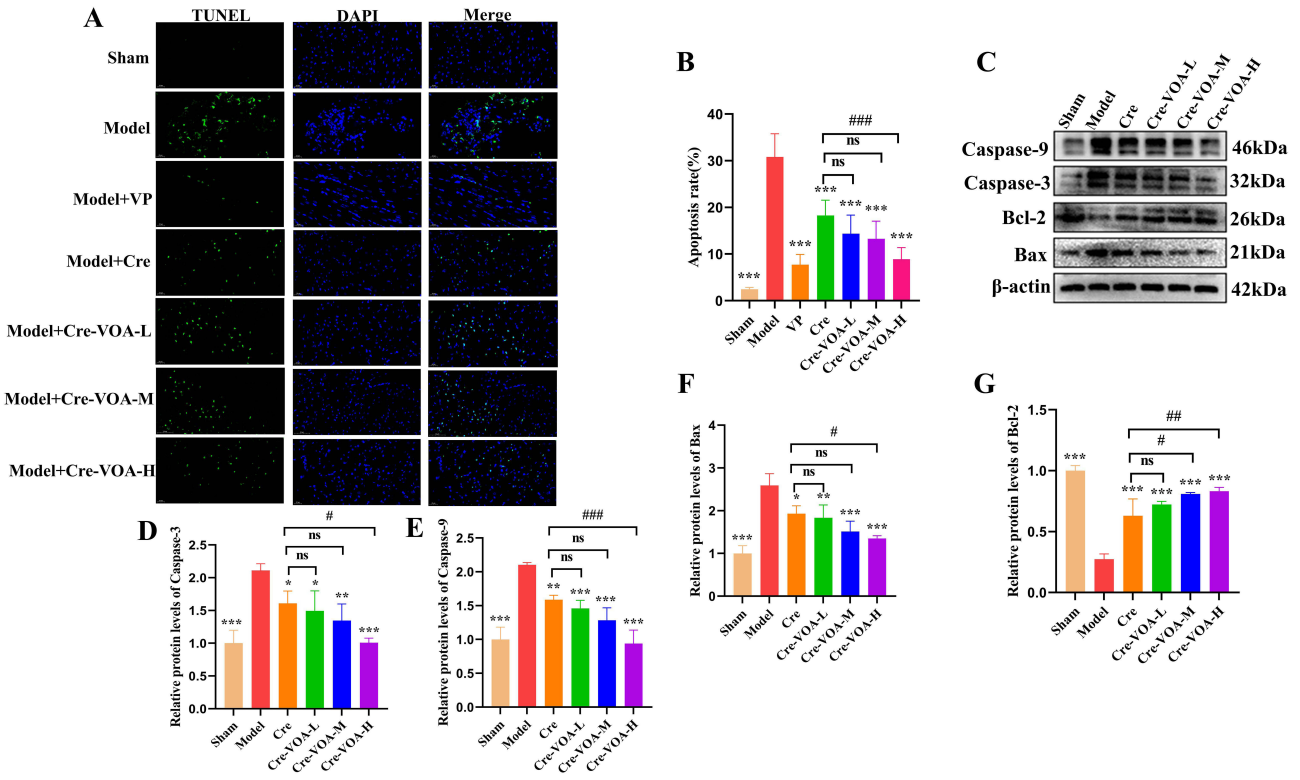

Figure 2 Cre and VOA administration resulted in decreased myocardial apoptosis of Model rats. (**A**)TUNEL assay to assess cell apoptosis rate (×400). (**B**)Quantitative analysis of apoptosis (n=6). (**C**)Western blot analysis of the relative protein expression (n=3). Relative protein expression of Caspase-3 (**D**), Caspase-9 (**E**), Bax (**F**), and Bcl-2 (**G**) is presented in bar graphs. *P < 0.05, **P < 0.01, ***P < 0.001 vs Model; #P < 0.05, ###P < 0.01, ###P < 0.001 vs Cre, ns indicates no significant difference.

Caspase-3, Caspase-9, and Bcl-2-associated protein (Bax), and upregulated the expression of the anti-apoptotic protein B-cell lymphoma-2 in myocardial tissues compared to the Model group (Figure 2C–G).

Cre and VOA Alleviate Endoplasmic Reticulum Stress Induced by MIRI

The expression of ERS-related proteins glucose-regulated protein 78 (GRP78), Activating Transcription Factor 6 (ATF6), Protein kinase RNA-like Endoplasmic Reticulum Kinase (PERK), and C/EBP homologous protein (CHOP) was assessed by Western blotting to investigate the effects of Cre and VOA pretreatment on ERS. The results showed that MIRI markedly upregulated GRP78, ATF6, PERK, and CHOP expression, whereas pretreatment with Cre and VOA significantly downregulated the expression levels of these proteins (Figure 3).

Cre and VOA Prevent Oxidative Stress and Inflammatory Responses in MIRI

The antioxidant properties of Cre and VOA were evaluated by measuring the serum levels of the oxidative stress marker MDA and the antioxidant enzyme SOD in rats. The results demonstrated that pretreatment with Cre and VOA significantly suppressed the I/R-induced increase in MDA levels and prevented the decrease in SOD activity (Figure 4A and B). Furthermore, ELISA and Western blot analyses revealed that, compared with the Sham group, I/R markedly increased the levels of TNF-α, IL-1β, and IL-6 and the phosphorylation of inflammation-related proteins p65 and p38. Pretreatment with Cre and VOA significantly reduced the expression of these cytokines and phosphorylated proteins (Figure 4C–I).

Effects of Cre and VOA Pretreatment on Serum Metabolites in MIRI Rats

Multivariate Statistical Analysis

To investigate the metabolic regulatory effects of Cre and VOA in MIRI, serum specimens from rat models underwent comprehensive metabolomic profiling and analytical procedures. Our findings revealed that

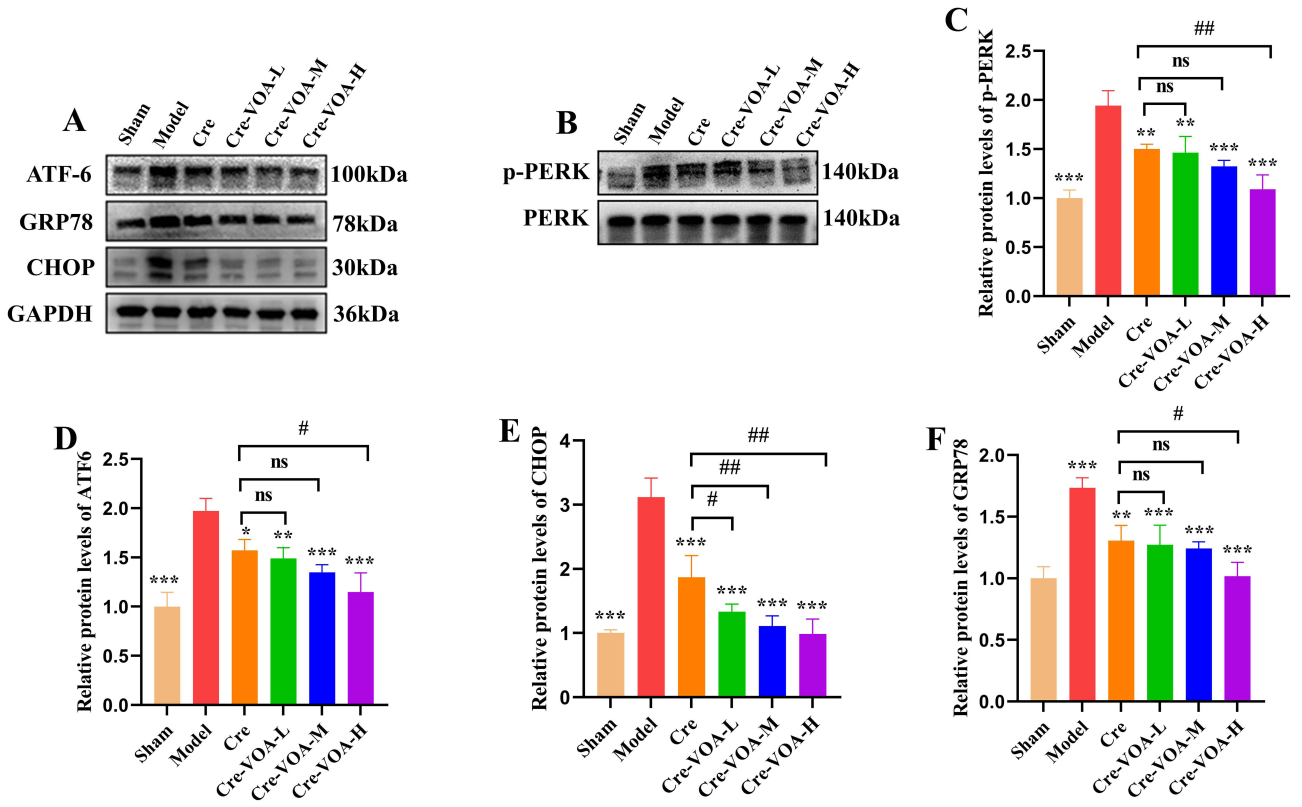

Figure 3 Cre and VOA Pretreatment Significantly Downregulates ERS-Related Protein Expression. (**A**) Representative immunoblots of ATF-6, GRP78, CHOP, and GAPDH. (**B**) Representative immunoblots of PERK and p-PERK. Relative protein expression of (**C**) p-PERK, (**D**) ATF-6, (**E**) CHOP, and (**F**) GRP78 is presented in bar graphs (n=3). *P < 0.05, **P < 0.01, ***P < 0.001 vs Model; #P < 0.05, ##P < 0.01, ###P < 0.001 vs Cre, ns indicates no significant difference.

characteristic chromatographic peaks demonstrated temporal consistency and signal magnitude alignment across measurements, indicating that experimental deviations arising from analytical system inconsistencies were statistically insignificant. PCA was used to evaluate the relationships in metabolomic distributions among the groups, and the results revealed significant intergroup separation and substantial intragroup aggregation in the Sham, Model, Cre, and Cre-V-M groups (Figure 5A–D). The evaluation parameters R2 and Q2 demonstrated good robustness of OPLS-DA without overfitting (Figure 5E and F). Therefore, it was suitable for metabolite and pathway analysis.

Analysis of Differential Metabolites of the Serum

The significance of metabolites across multiple groups was first analyzed using a one-way ANOVA. Differentially expressed metabolites across experimental groups were identified using an OPLS-DA model, with selection criteria set at p-value < 0.05 (P < 0.05) and VIP > 1. After screening, we identified 75 significant differential metabolites in MIRI regulated by Cre and VOA. These metabolites were significantly reverted in the serum of rats in the Cre and Cre-V-M groups, compared with the Model group.

Compared to the Model group, the Cre group indicated upregulation of 11 metabolites and downregulation of 17 metabolites (Table 2), and the Cre-V-M group showed upregulation of 16 metabolites and downregulation of 31 metabolites (Table 3). Of the 75 significant differential metabolites, 13 were affected by Cre and Cre-V-M. Compared to the Model group, seven metabolites were downregulated (phosphatidylinositol lyso 20, methyl palmitoleate, oleic acid, norstictic acid, 9-trans-palmitelaidic Acid, dihydroxyheptadec-16-enyl acetate, roccellic acid), and six metabolites were upregulated (butyl paraben, L-glutamic acid, gluconate, 3-indoxyl sulfate, D-pantothenic acid, atrazine). Moreover, Cre-V-M exhibited better regulatory effects than Cre (Table 4).

https://doi.org/10.2147/JIR.S527105

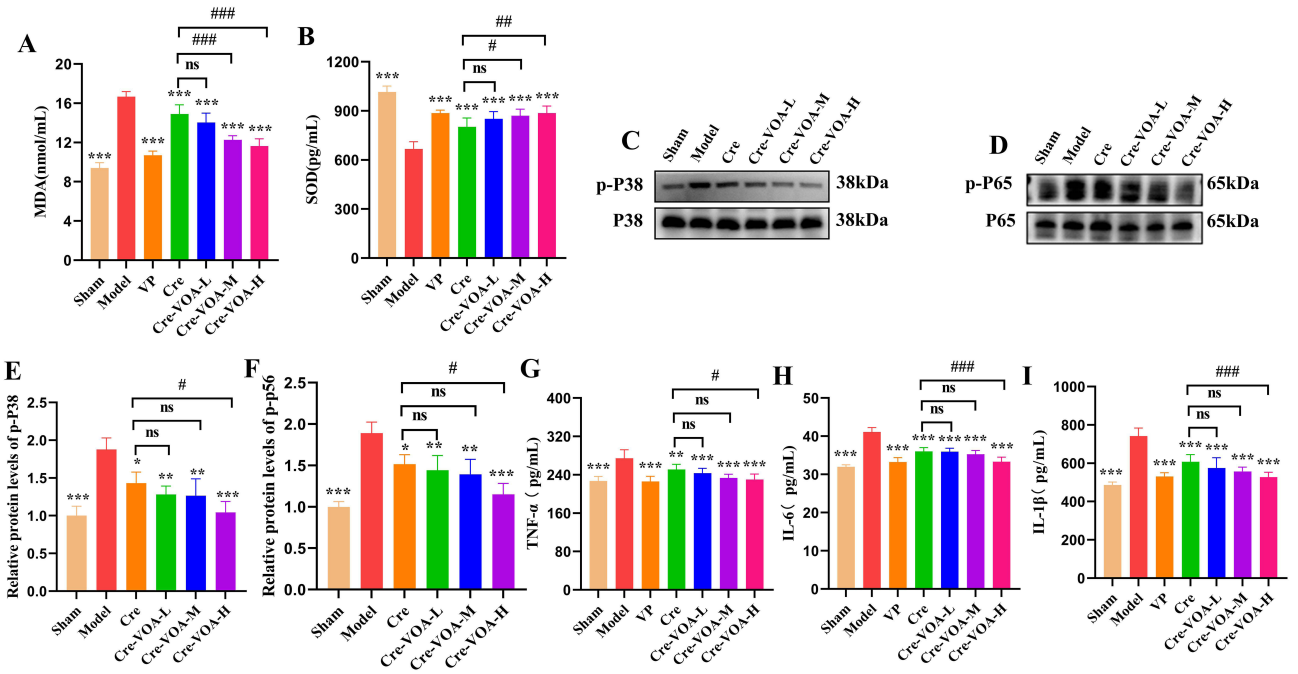

Figure 4 Cre and VOA can alleviate Oxidative Stress and myocardial inflammatory Responses caused by MIRI. The (**A**) MDA levelsand (**B**)SOD levels in ischemic cardiac tissue (n = 6). (**C** and **D**) The expression levels of Inflammation-related proteins (p-p38, p-p65) were analyzed via Western blotting. Relative protein expression of (**E**)p-p38 and (**F**)p-p65 (n=3). Serum levels of (**G**)TNF-α, (**H**)IL-6, and (**I**)IL-1β (n = 6). *P < 0.05, **P < 0.01, ***P < 0.001 vs Model; #P < 0.05, ##P < 0.01, ###P < 0.001 vs Cre, ns indicates no significant difference.

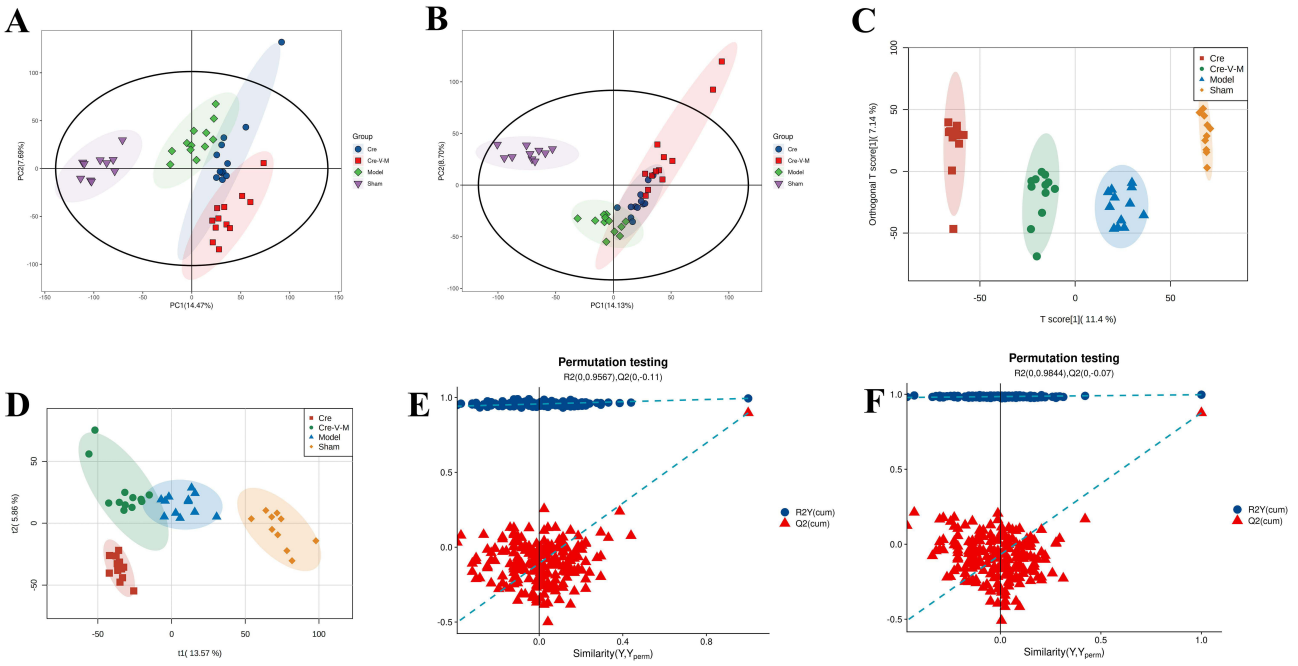

Figure 5 Model analysis of the effectiveness and reliability of metabolomics. PCA of serum samples from each group (**A** and **B**). OPLS-DA scores of serum samples in each group (**C** and **D**). OPLS–DA permutation test for serum samples from each group (E-F), ((**A, C** and **E**) Positive Ion Mode; (**B, D** and **F**) Negative Ion Mode).

Metabolic Pathway Analysis

Our study of the metabolic pathways of potential biomarkers revealed that Cre primarily affects the serum metabolism of model rats by regulating six metabolic pathways: biosynthesis of cofactors, the pentose phosphate pathway, β-alanine

Table 2 Differential Metabolites Information Table Between Cre and Model Groups

MetaboName	RT (min)	m/z	Adduct type	Formula	Trend	
					Model/Sham	Cre/Model
5-Fluro-2-Pyrimidone	1.37	115.04	$[M^+Na]^+$	$C_4H_3FN_2O$	↑	↓
Nicotinamide	2.59	123.06	$[M^+H]^+$	$C_6H_6N_2O$	↑	↓
2-Phenylacetamide	3.91	136.08	$[M^+H]^+$	C_8H_9NO	↓	↑
Tyrosine	3.91	182.08	$[M^+H]^+$	$C_9H_{11}NO_3$	↓	↑
L-Tryptophan	5.28	205.10	$[M^+H]^+$	$C_{11}H_{12}N_2O_2$	↓	↑
Chaulmoogric Acid	11.47	281.25	$[M^+H]^+$	$C_{18}H_{32}O_2$	↑	↓
Dibromo, Dimethylether, Hydroxypinoresinol	6.39	559.00	$[M^+H]^+$	$C_{22}H_{24}Br_2O_7$	↑	↓
Cimicidanol-3-O-Alpha-L-Arabinoside	6.46	617.36	$[M^+2H]^{2+}$	$C_{35}H_{52}O_9$	↑	↓
Taurohyodeoxycholic Acid	7.17	498.29	$[M^-H]^-$	$C_{26}H_{45}NO_6S$	↓	↑
LPE 16:0	9.58	452.28	$[M^-H]^-$	$C_{21}H_{44}NO_7P$	↑	↓
Phosphatidylethanolamine Lyso Alkenyl 16	9.85	436.28	$[M^-H]^-$	$C_{21}H_{44}NO_6P$	↑	↓
Docosatetraenoic Acid	11.89	331.26	$[M^-H]^-$	$C_{22}H_{36}O_2$	↑	↓
2,4-Dihydroxyheptadec-16-Enyl Acetate	12.10	327.25	$[M^-H]^-$	$C_{19}H_{36}O_4$	↑	↓
Docosahexanoic Acid	11.16	327.23	$[M^-H]^-$	$C_{22}H_{32}O_2$	↑	↓
Eicosenoic Acid	13.13	309.28	$[M^-H]^-$	$C_{20}H_{38}O_2$	↑	↓
Abietic Acid	10.90	301.22	$[M^-H]^-$	$C_{20}H_{30}O_2$	↑	↓
Oleic Acid	13.01	281.25	$[M^-H]^-$	$C_{18}H_{34}O_2$	↑	↓
Linoleic Acid	11.47	279.23	$[M^-H]^-$	$C_{18}H_{32}O_2$	↑	↓
Y-Linolenic Acid	11.00	277.22	$[M^-H]^-$	$C_{18}H_{30}O_2$	↑	↓
9-Trans-Palmitelaidic Acid	11.28	253.22	$[M^-H]^-$	$C_{16}H_{30}O_2$	↑	↓
D-Pantothenic Acid	5.14	218.10	$[M^-H]^-$	$C_9H_{17}NO_5$	↓	↑
Atrazine	5.78	214.00	$[M^-H]^-$	$C_8H_{14}ClN_5$	↓	↑
3-Indoxyl Sulfate	5.78	212.00	$[M^-H]^-$	$C_8H_7NO_4S$	↓	↑
Tryptophan	5.28	203.08	$[M^-H]^-$	$C_{11}H_{12}N_2O_2$	↓	↑
Gluconate	1.28	195.05	$[M^-H]^-$	$C_6H_{12}O_7$	↓	↑
Citrate	2.13	191.02	$[M^-H]^-$	$C_6H_8O_7$	↓	↑
L-Histidine	1.24	154.06	$[M^-H]^-$	$C_6H_9N_3O_2$	↑	↓
Glyceraldehyde	2.09	89.02	$[M^-H]^-$	$C_3H_6O_3$	↓	↑

Table 3 Differential Metabolites Information Table Between Cre-V-M and Model Group

MetaboName	RT (min)	m/z	Adduct Type	Formula	Trend	
					Model/Sham	Cre-V-M/Model
Desferrioxamine G1	6.46	619.37	$[M^{+2}H]^{2+}$	$C_{27}H_{50}N_6O_{10}$	↑	↓
Puwainaphycin D	6.46	613.36	$[M^+H^-2H2O]^+$	$C_{57}H_{97}ClN_{12}O_{15}$	↑	↓
Desmethylenylnocardamine	6.45	604.36	$[M^+NH^4]^+$	$C_{26}H_{46}N_6O_9$	↑	↓
Polyphyllin A	6.45	599.36	$[M^+NH^4]^+$	$C_{33}H_{52}O_8$	↑	↓
Dibromo, Dimethylether, Hydroxypinoresinol	6.39	559.00	$[M^+H]^+$	$C_{22}H_{24}Br_2O_7$	↑	↓
Hypaconine	6.23	470.27	$[M^+2H]^{2+}$	$C_{24}H_{39}NO_8$	↑	↓
Ranolazine Dihydrochloride	6.23	428.26	$[M^+NH^4]^{2+}$	$C_{24}H_{33}N_3O_4$	↑	↓
Bonactin	6.14	401.26	$[2M^+H]^+$	$C_{21}H_{36}O_7$	↑	↓
Corticosterone	7.67	347.22	$[M^+H]^+$	$C_{21}H_{30}O_4$	↑	↓
Cimicidanol-3-O-Alpha-L-Arabinoside	6.46	617.36	$[M^{+2}H]^{2+}$	$C_{35}H_{52}O_9$	↑	↓
Icos-19-Ene-1,2,4-Triol	8.34	346.33	$[M^+NH^4]^+$	$C_{20}H_{40}O_3$	↑	↓
Dehydroabietamide	7.59	300.20	$[M^+NH^4]^+$	$C_{20}H_{29}NO$	↑	↓
Jaeschkeanadiol	8.95	256.23	$[M^+H]^+$	$C_{15}H_{26}O_2$	↑	↓
Pantothenic Acid	5.14	220.12	$[M^+H]^+$	$C_9H_{17}NO_5$	↓	↑

(*Continued*)

Table 3 (Continued).

MetaboName	RT (min)	m/z	Adduct Type	Formula	Trend	
					Model/Sham	Cre-V-M/Model
L-Tryptophan	5.28	205.10	$[M^+H]^+$	$C_{11}H_{12}N_2O_2$	↓	↑
6-Ethoxy-2-Mercaptobenzothiazole	7.61	212.02	$[M^+H]^+$	$C_9H_9NOS_2$	↓	↑
Acetylcarnitine	1.41	204.12	$[M]^+$	$C_9H_{18}NO_4$	↑	↓
Theobromine	1.28	203.05	$[M^+Na]^+$	$C_7H_8N_4O_2$	↓	↑
Tyrosine	3.91	182.08	$[M^+H]^+$	$C_9H_{11}NO_3$	↓	↑
3-Indoleacetic Acid	6.79	176.07	$[M^+H]^+$	$C_{10}H_9NO_2$	↑	↓
Vanillin	5.02	153.07	$[M^+H]^+$	$C_8H_8O_3$	↑	↓
Glutamic Acid	1.29	148.06	$[M^+H]^+$	$C_5H_9NO_4$	↓	↑
Phenethylamine	9.93	122.11	$[M^+H]^+$	$C_8H_{11}N$	↓	↑
Benzamidine	1.32	121.07	$[2M^+H]^+$	$C_7H_8N_2$	↑	↓
Indole-3-Carboxyaldehyde	5.28	146.06	$[M^+H]^+$	C_9H_7NO	↑	↓
Phosphatidylcholine Lyso 18	10.16	552.37	$[M^+Hac^-H]^-$	$C_{26}H_{52}NO_7P$	↑	↓
LPE 16:0	9.58	452.28	$[M^-H]^-$	$C_{21}H_{44}NO_7P$	↑	↓
Dehydrorotenone	7.67	391.21	$[M^-H]^-$	$C_{23}H_{20}O_6$	↑	↓
Docosatetraenoic Acid	11.89	331.26	$[M^-H]^-$	$C_{22}H_{36}O_2$	↑	↓
2,4-Dihydroxyheptadec-16-Enyl Acetate	12.10	327.25	$[M^-H]^-$	$C_{19}H_{36}O_4$	↑	↓
Avocadyne Acetate	11.47	325.24	$[M^-H]^-$	$C_{19}H_{34}O_4$	↑	↓
Eicosenoic Acid	13.13	309.28	$[M^-H]^-$	$C_{20}H_{38}O_2$	↑	↓
Trans-Vaccenic Acid	12.10	281.25	$[M^-H]^-$	$C_{18}H_{34}O_2$	↑	↓
Oleic Acid	13.01	281.25	$[M^-H]^-$	$C_{18}H_{34}O_2$	↑	↓
Palmitic Acid	11.99	255.23	$[M^-H]^-$	$C_{16}H_{32}O_2$	↑	↓
9-Trans-Palmitelaidic Acid	11.28	253.22	$[M^-H]^-$	$C_{16}H_{30}O_2$	↑	↓
D-Pantothenic Acid	5.14	218.10	$[M^-H]^-$	$C_9H_{17}NO_5$	↓	↑
Atrazine	5.78	214.00	$[M^-H]^-$	$C_8H_{14}ClN_5$	↓	↑
3-Indoxyl Sulfate	5.78	212.00	$[M^-H]^-$	$C_8H_7NO_4S$	↓	↑
Tryptophan	5.28	203.08	$[M^-H]^-$	$C_{11}H_{12}N_2O_2$	↓	↑
Gluconate	1.28	195.05	$[M^-H]^-$	$C_6H_{12}O_7$	↓	↑
Pyridoxine	2.74	168.02	$[M^-H]^-$	$C_8H_{11}NO_3$	↓	↑
Urate	2.75	167.02	$[M^-H]^-$	$C_5H_4N_4O_3$	↓	↑
L-Histidine	1.24	154.06	$[M^-H]^-$	$C_6H_9N_3O_2$	↑	↓
2-Hydroxybenzaldehyde	6.78	121.03	$[M^-H]^-$	$C_7H_6O_2$	↑	↓
Purine	1.30	119.03	$[M^-H]^-$	$C_5H_4N_4$	↓	↑
2-Oxobutyric Acid	1.30	101.02	$[M^-H_2O^-H]^-$	$C_4H_6O_3$	↓	↑

metabolism, biosynthesis of unsaturated fatty acids, biosynthesis of amino acids, and phenylalanine, tyrosine, and tryptophan biosynthesis.

VOA and Cre mainly regulate the serum metabolism of rat models through nine metabolic pathways: β-alanine metabolism, the pentose phosphate pathway, biosynthesis of unsaturated fatty acids, glutathione metabolism, biosynthesis of amino acids, tryptophan metabolism, glycine, serine, and threonine metabolism, biosynthesis of cofactors and 2-oxocarboxylic acid metabolism. The Cre and Cre-V-M groups regulate five metabolic pathways in common, with four additional metabolic pathways regulated by the Cre-V-M group compared to the Cre group. These results indicate that the synergistic effect of VOA with Cre enhances Cre's regulation of the metabolic pathways in model rats, alleviating MIRI. Detailed results are shown in Figure 6.

Discussion

This study contributes to elucidating the potential mechanisms by which Cre and VOA exert protective effects against MIRI, with the following major findings: (1) Cre and VOA reduced myocardial infarct size and alleviated

Table 4 Cre and Cre-V-M Group Common Differential Metabolites Information Table

Metabolites	RT (min)	m/z	Adduct Type	Formula	Trend Cre/Model Cre-V-M/Model
Butyl Paraben	1.35	233.06	$[M^+NH_4]^+$	$C_{11}H_{14}O_3$	↑ ↑
Roccellic Acid	11.28	299.22	$[M^-H]^-$	$C_{17}H_{32}O_4$	↓ ↓
Phosphatidylinositol Lyso 20	13.41	619.29	$[M^+Hac^-H]^-$	$C_{29}H_{49}O_{12}P$	↓ ↓
Oleic Acid	13.01	281.25	$[M^-H]^-$	$C_{18}H_{34}O_2$	↓ ↓
Norstictic Acid	2.87	371.01	$[M^-H]^-$	$C_{18}H_{12}O_9$	↓ ↓
Methyl Palmitoleate	11.68	267.23	$[M^-H]^-$	$C_{17}H_{32}O_2$	↓ ↓
L-Glutamic Acid	2.33	128.03	$[M^-H]^-$	$C_5H_7NO_3$	↑ ↑
Gluconate	1.28	195.05	$[M^-H]^-$	$C_6H_{12}O_7$	↑ ↑
Atrazine	5.78	214.00	$[M^-H]^-$	$C_8H_{14}ClN_5$	↑ ↑
9-Trans-Palmitelaidic Acid	11.28	253.22	$[M^-H]^-$	$C_{16}H_{30}O_2$	↓ ↓
3-Indoxyl Sulfate	5.78	212.00	$[M^-H]^-$	$C_8H_7NO_4S$	↑ ↑
2,4-Dihydroxyheptadec-16-Enyl Acetate	12.10	327.25	$[M^-H]^-$	$C_{19}H_{36}O_4$	↓ ↓
D-Pantothenic Acid	5.14	218.10	$[M^-H]^-$	$C_9H_{17}NO_5$	↑ ↑

histopathological damage induced by I/R; (2) Cre and VOA attenuated ERS-induced apoptosis by inhibiting the activation of the GRP78-PERK/ATF6-CHOP signaling pathway; (3) Cre and VOA suppressed excessive activation of the Mitogen-activated protein kinase/nuclear factor kappa B/tumor necrosis factor-alpha (MAPK-NF-κB-TNF-α) pathway, thereby mitigating inflammation driven by ERS and oxidative stress. These findings suggest that Cre combined with VOA can alleviate MIRI, providing further evidence to support the cardioprotective properties of Cre.

Multiple pathological factors, including oxidative stress, ERS, apoptosis, and inflammatory response, can trigger MIRI. Oxidative stress is considered one of the most critical mechanisms underlying MIRI. It leads to irreversible myocardial cell damage and cardiac dysfunction by promoting cardiomyocyte apoptosis, ERS, and inflammation through various pathways. During the reperfusion phase, excessive generation of ROS leads to a reduction in endogenous ROS scavengers, such as SOD, catalase, and glutathione, resulting in a redox imbalance and initiation of lipid peroxidation cascades that disrupt cellular structures and cause myocardial injury.[25] In addition, overproduction of ROS elevates MDA levels, which is a key biomarker of oxidative stress. Therefore, we evaluated the antioxidant effects of Cre and VOA by measuring serum SOD and MDA levels. The results demonstrated that oral pretreatment with Cre and VOA significantly reduced MDA levels and increased SOD activity in model rats, thereby suppressing oxidative stress.

During myocardial I/R, oxidative stress can trigger ERS and activate downstream apoptotic pathways. During reperfusion, factors such as hypoxia, calcium overload, and insufficient energy supply disrupt ER homeostasis, leading to the accumulation of unfolded or misfolded proteins, a condition known as the unfolded protein response, which initiates ERS.[26,27] Under normal conditions, the chaperone immunoglobulin heavy chain binding protein/GRP78 binds to three primary ERS sensors: IRE1, PERK, and ATF6.[28] However, GRP78 exhibits a higher affinity for unfolded/misfolded proteins, resulting in its dissociation from these sensors and subsequent activation of ERS signaling pathways.[29] Thus, GRP78 is widely recognized as a marker of ERS.

Moreover, ERS disrupts redox homeostasis, promotes ROS accumulation, and impairs mitochondrial function, ultimately exacerbating cardiomyocyte apoptosis.[30] Prolonged ERS induces apoptosis through pathways mediated by activated PERK and ATF6, which upregulate CHOP, a pro-apoptotic transcription factor.[31,32] CHOP further promotes the activation of downstream apoptotic signaling. Oxidative stress and ERS can increase mitochondrial Ca^{2+} uptake, trigger the opening of the mitochondrial permeability transition pore, disturb membrane potential, and lead to the release of apoptotic signaling molecules, such as apoptosis-inducing factor.[33–36] In the cytoplasm, apoptosome formation occurs via cytochrome c, apoptotic protease-activating factor-1, and caspase-9, which subsequently activates caspase-3, ultimately executing the apoptotic cascade.[33,35] In this study, we assessed the expression of ERS-related proteins (GRP78, PERK, ATF6, CHOP) and apoptotic markers (caspase-9, Bcl-2, caspase-3, and Bax). Our findings suggest that Cre and VOA mitigate ERS–induced apoptosis by modulating the GRP78-PERK/ATF6-CHOP signaling pathway.

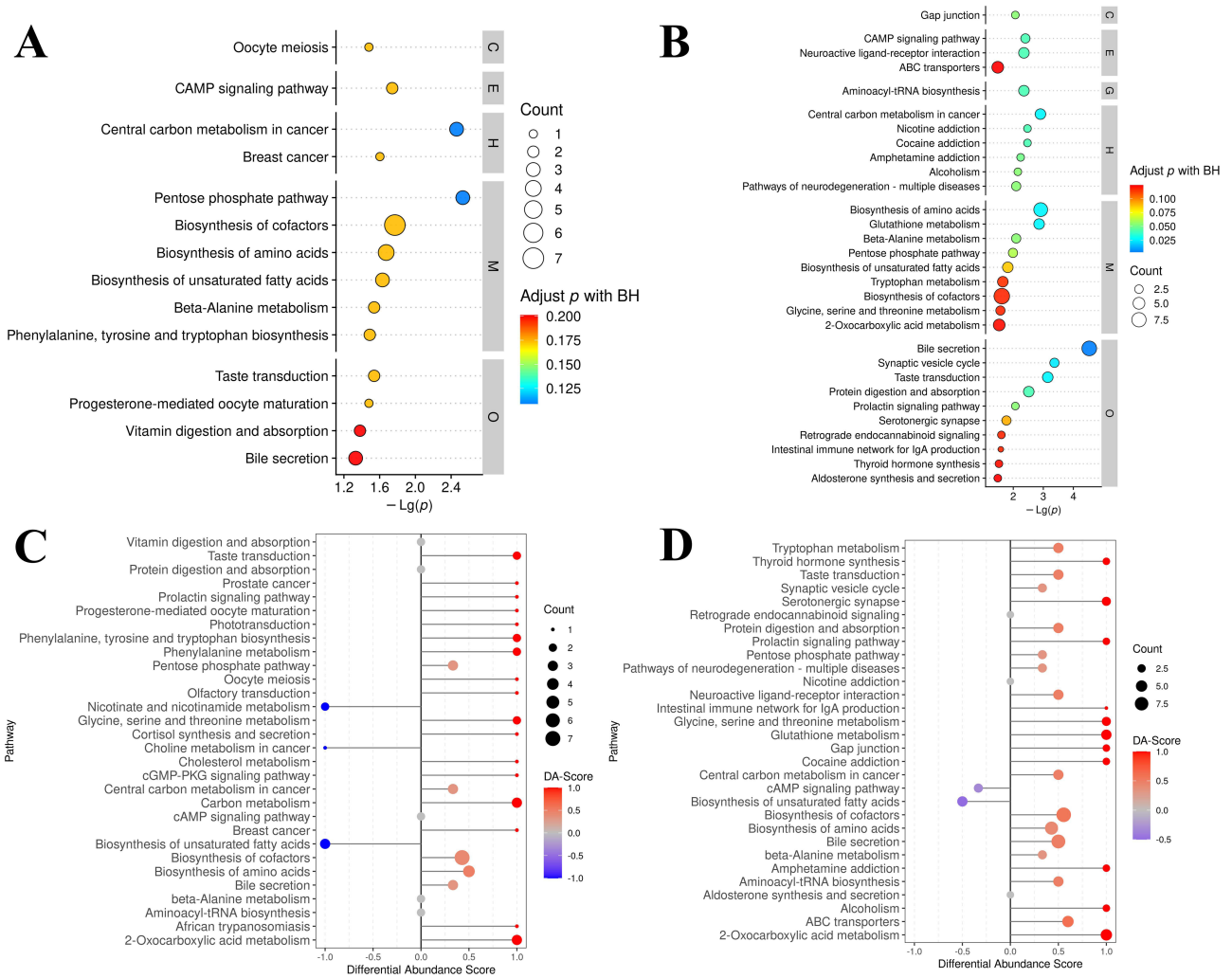

Figure 6 Metabolic pathways analysis. KEGG pathways enrichment bubble map. (size and color of circles represent gene counts and adjusted p-values in the pathway, respectively); DA score demonstrates overall up- and down-regulation of metabolic pathways. (The color of circles from blue to red represent DA score from −1 to 1, indicating that the overall expression of the pathway tends to be more down-regulated (−1) or up-regulated (1).) ((**A** and **C**): Cre group vs Model group; (**B** and **D**): Cre-V-M group vs Model group).

Previous studies have demonstrated that oxidative stress and ERS can activate inflammatory responses through apoptosis, thereby exacerbating MIRI. MAPKs are a family of proteins activated by ROS. ROS-induced MAPKs, particularly p38 and Janus kinase, initiate the extrinsic cell death cascade through the MAPK-NF-κB-TNF-α signaling pathway.[25] In addition, caspase-3 expression upregulates phosphorylated p38 MAPK (p-p38 MAPK).[37] Adenosine monophosphate-activated protein kinase (AMPK) can attenuate inflammatory responses by inhibiting oxidative stress through antioxidant mechanisms. Activation of AMPK regulates the p38 MAPK signaling pathway, and activated p38 MAPK further stimulates NF-κB, promoting the synthesis and secretion of proinflammatory cytokines. Thus, the p38 signaling cascade mediates inflammatory responses and mitochondrial apoptosis during myocardial ischemia.[38,39] Consistent with these findings, our study revealed that Cre and VOA may suppress the excessive activation of the MAPK-NF-κB-TNF-α signaling axis by downregulating caspase-9 and caspase-3 expression by modulating ERS and oxidative stress. This multi-targeted mechanism effectively attenuates oxidative damage, inhibits the release of inflammatory cytokines and cardiomyocyte programmed death, and ultimately reduces the extent of myocardial tissue injury induced by I/R.

In addition, non-targeted metabolomics analysis was conducted on serum samples from each group. The results revealed that Cre and VOA reduced serum levels of oleic acid in rat models and elevated the levels of metabolites, such

as L-Glutamic Acid, gluconate, and pantothenic acid. These treatments also regulate the glycine, serine, and threonine metabolism, glutathione metabolism, pentose phosphate pathway and enhance biosynthesis of confactor, β-alanine metabolism, tryptophan metabolism, 2-oxocarylic acid metabolism and amino acid biosynthesis. Meanwhile, the biosynthesis of unsaturated fatty acids was suppressed. These altered pathways are closely associated with glucose-lipid and amino acid metabolism.

Normal myocardial function requires substantial ATP consumption, and MIRI is tightly regulated the metabolism of energy substrates. Glucose, fatty acids, and amino acids are primary energy substrates for the heart. However, I/R disrupts energy metabolism, leading to metabolic imbalance, which ultimately results in cell death and impaired cardiac function. Restoring the balance between glucose and lipid metabolism and correcting abnormal myocardial energy metabolism represents a promising strategy for mitigating MIRI.[40]

The tricarboxylic acid (TCA) cycle is a primary mitochondrial pathway for ATP production, playing a critical role in myocardial energy metabolism. An increasing body of research has indicated that the TCA cycle regulates NADH/NADPH homeostasis, scavenges ROS, generates ATP through substrate-level phosphorylation, participates in signal transduction, and supplies intermediates to counteract cellular stress responses.[41] The glycine, serine, and threonine metabolism pathway provides key metabolic precursors that fuel the TCA cycle.[42] Pantothenic acid and threonine are precursors of coenzyme A (CoA), which can be converted into acetyl-CoA to enter the TCA cycle.[43] CoA is also essential for lipid metabolism, particularly for the transport of fatty acids from the cytosol to the mitochondria. Furthermore, decreased pantothenic acid levels have been proposed as a biomarker for lipid and energy metabolism disorders.[44] Our findings revealed that Cre and VOA enhanced glycine, serine, and threonine metabolism and increased serum pantothenic acid levels in rats subjected to MI/R. These changes may promote TCA cycle activity, thereby supporting myocardial energy homeostasis and facilitating the clearance of excess ROS.

Glutamic acid is a vital energy source for cardiomyocytes. Under hypoxic conditions, glutamate consumption increases, leading to a reduction in myocardial glutamate levels.[45] Elevated intracellular glutamate levels improve calcium homeostasis and enhance resistance to oxidative stress.[46,47] Glutamic acid also contributes to myocardial protection during ischemia-reperfusion by promoting glycogen synthesis and activating the AMPK pathway, which enhances glycolysis, thereby alleviating MIRI.[48] Glutamic acid serves as a rate-limiting precursor for glutathione (GSH) synthesis. GSH, composed of glutamate, cysteine, and glycine, is a major intracellular antioxidant and redox regulator.[46,47,49] In addition, glutamic acid is a key anaerobic substrate in the TCA cycle. It can be converted to alpha-ketoglutaric acid via transaminase or glutamate dehydrogenase, thereby feeding into the TCA cycle and contributing to ATP production, which supports cardioprotection.[50] Our findings suggest that Cre and VOA may exert cardioprotective effects during MI/R by enhancing glutathione metabolism and increasing serum glutamic acid levels, thus helping to maintain cellular energy homeostasis and combat oxidative stress.

Oleic acid (OA), a monounsaturated fatty acid, is implicated in the impairment of mitochondrial function in cardiomyocytes. Elevated circulating levels of OA are associated with an increased risk of adverse cardiovascular events and appear to be independent of dietary intake.[51] During I/R, OA levels increase due to the oxygen-intensive nature of its catabolism. The sharp decline in oxygen supply during ischemia impairs OA degradation, and fatty acid utilization by cardiomyocytes is reduced under ischemic conditions, resulting in a relative accumulation of OA.[52]

Consistent with previous findings, our study demonstrated a significant elevation of OA in the serum of rats subjected to I/R, which was restored to normal levels following treatment with Cre and VOA. Previous studies have shown that OA promotes the production of ROS.[53] Therefore, Cre and VOA may exert cardioprotective effects by suppressing the biosynthesis of unsaturated fatty acids, thereby reducing serum OA levels in I/R-injured rats, which limits ROS generation, alleviating oxidative and ER stress, and ultimately reduces myocardial injury.

The pentose phosphate pathway, a pivotal glucose metabolic route, plays crucial roles in reductive biosynthesis, nucleotide synthesis, and the prevention of oxidative stress by generating NADPH and ribose-5-phosphate.[54] NADPH, a reducing agent, prevents ROS production.[55] MIRI is mediated by various factors, including increased ROS generation, especially during reperfusion.[56] ROS mediates MIRI in two primary ways. First, ROS initiates cascade lipid peroxidation, thereby disrupting cellular architecture and physiological functions, ultimately resulting in apoptosis and necrosis.[57–59] This increases the serum levels of lipid peroxidation products and the activity of antioxidant enzymes,

such as SOD, ultimately inducing myocardial damage. Second, ROS serves as a stimulatory signal for NF-κB activation, which triggers inflammation and injury by upregulating Bax, TNF-α, and transforming growth factor-beta1. The generation of ROS and induction of NF-κB are vital determinants of the severity of myocardial injury.[60,61] Our experimental findings validate these pathogenic mechanisms and demonstrate that Cre combined with VOA ameliorates IR-induced myocardial inflammation and apoptosis by modulating the pentose phosphate pathway.

Energy metabolism plays a pivotal role in the regulation of oxidative stress, inflammation, and ERS. Based on our metabolomics findings and previous experimental data, Cre and VOA exert their protective effects primarily by enhancing the pentose phosphate pathway, glutathione metabolism, and glycine, serine, and threonine metabolism while increasing the serum levels of glutamic and pantothenic acids. Simultaneously, they suppress the biosynthesis of unsaturated fatty acids, particularly serum oleic acid. These changes collectively modulate antioxidant pathways, inhibit ROS generation during MI/R, and promote ROS elimination.

Energy metabolism regulates oxidative and ER stress by balancing ROS production and clearance. During I/R, ROS levels are markedly elevated. Cre and VOA may reduce ROS production through improved energy metabolism, elevate serum levels of antioxidant enzymes, such as SOD and glutathione, and facilitate the scavenging of excessive ROS. This ultimately suppresses oxidative stress and lowers MDA levels, a marker of oxidative injury. Cre and VOA can also modulate the dynamic levels of ROS through metabolic regulation, and may indirectly inhibit ERS through the GRP78-PERK/ATF6-CHOP signaling pathway.

Our study provides preliminary evidence supporting the synergistic cardioprotective effects of Cre and VOA against MIRI; however, several limitations should be acknowledged. First, the investigation was restricted to the acute phase of MIRI. Second, functional validation of cardiac performance parameters was not performed. Third, while the metabolomics

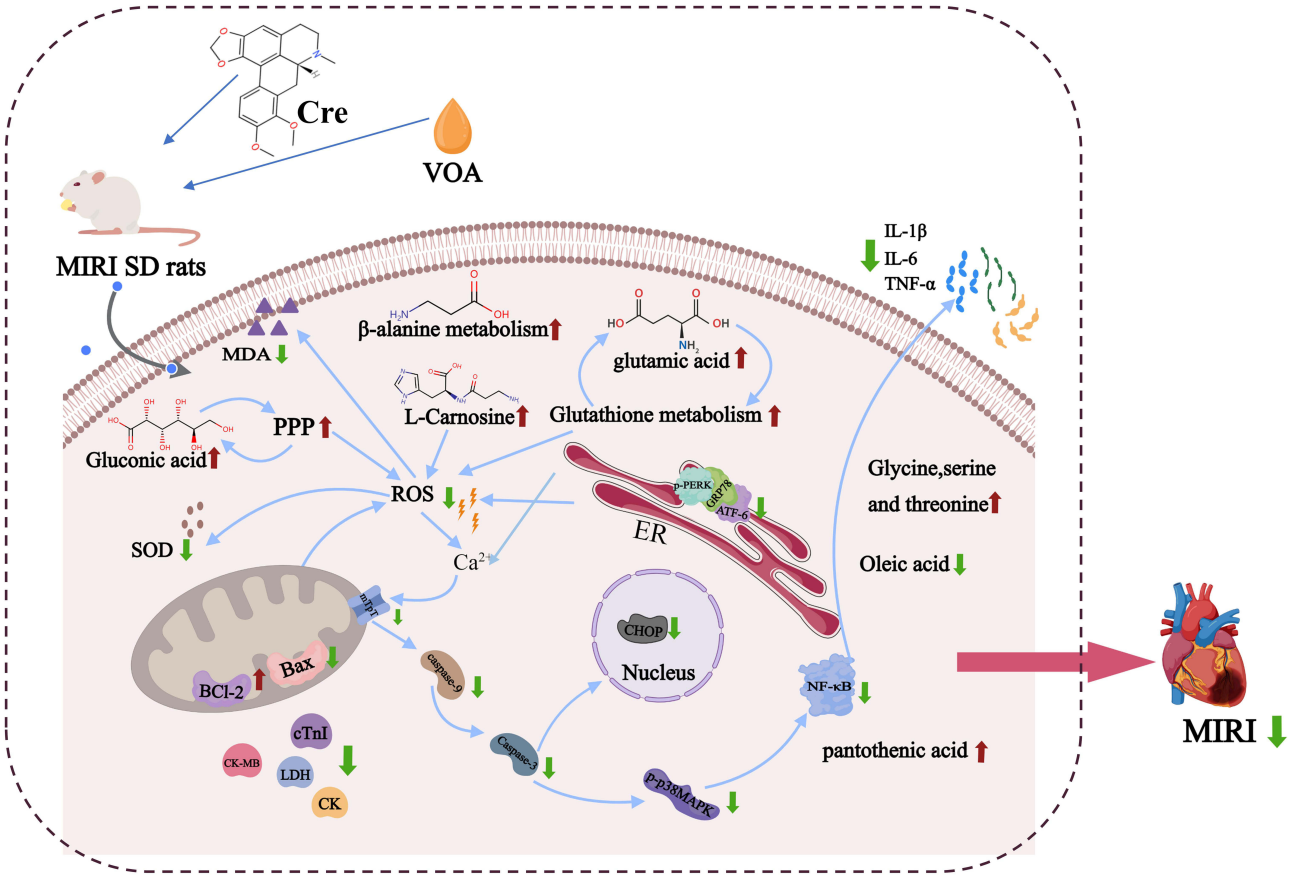

Figure 7 Schematic diagram of the mechanism of VOA synergizing with Cre to attenuate MIRI injury. Cre and VOA may attenuate myocardial ischemia-reperfusion injury by regulating energy metabolism and suppressing oxidative stress and endoplasmic reticulum (ER) stress-induced apoptosis and inflammation. These effects are mediated primarily through the GRP78-PERK/ATF6-CHOP and MAPK-NF-κB-TNF-α signaling pathways.

data are intrinsically relevant to the study, no direct causal relationships were experimentally verified. These limitations warrant further investigations. Future studies should explore whether Cre and VOA exert protective effects throughout the entire course of MIRI. In addition, the hypotheses derived from the metabolomic findings should be validated through targeted mechanistic studies to provide valuable insights into the therapeutic potentials of Cre and VOA.

Conclusion

This study provides scientific evidence that Cre and VOA may alleviate MIRI by modulating energy metabolism and suppressing oxidative stress and ERS-induced apoptosis and inflammatory responses through the GRP78-PERK/ATF6-CHOP and MAPK–NF-κB–TNF-α signaling pathways (Figure 7). Given the multifactorial pathogenesis of MIRI, VOA and Cre offers a promising multi-targeted therapeutic approach for mitigating myocardial damage. Previous pharmacokinetic studies conducted by our group have demonstrated that VOA significantly enhances the myocardial distribution of Cre. Consistent with this finding, this present study demonstrates that VOA facilitates the "targeting to the heart" effect, thereby amplifying the cardioprotective efficacy of Cre. These preclinical findings suggest that the combined use of VOA and Cre holds translational potential for the treatment of MIRI.

Future studies may benefit from integrating metabolomic data with extended observation time points (such as 24 h, 7 days, or 1 month post-reperfusion) to assess the therapeutic efficacy of the VOA-Cre combination in the acute to chronic phases of MIRI. Such investigations will provide a more comprehensive understanding of the synergistic cardioprotective effects of these compounds.

Abbreviations

Cre, Crebanine; VOA, Volatile oil from *Acorus gramineus* rhizoma; VP, Verapamil; MI, Myocardial ischemia; I/R, Ischemia/reperfusion; Myocardial ischemia reperfusion, MI/R; MIRI, Myocardial ischemia-reperfusion injury; UPR, Unfolded protein response; ERS, Endoplasmic reticulum stress; ER, Endoplasmic reticulum; IL-6, Interleukin-6; IL-1β, Interleukin-1β; SOD, Superoxide dismutase; cTnI, Cardiac troponin I; TNF-α, Tumor necrosis factor-α; LDH, Lactate dehydrogenase; MDA, Malondialdehyde; CK-MB, Creatine kinase-MB isoenzyme; CK, Creatine kinase; ROS, Reactive oxygen species; TCM, Traditional chinese medicine; ATP, Adenosine triphosphate.

Data Sharing Statement

All the data used in this study are available from the corresponding author upon reasonable request.

Ethical Approval and Informed Consent

This research was authorized by the Ethics Committee for Animal Research at the Traditional Chinese Medicine University in Yunnan. As indicated by approval number R-062022005. Additionally, the experiment complied with China's Guidelines for the Welfare and Ethical Review of Laboratory Animals (Standard No. GB/T 35892-2018).

Consent for Publication

Each author has reviewed and consented to the manuscript's content, with unanimous endorsement of its finalized version.

Acknowledgments

We sincerely thank the researchers for their contributions and the support from the Key R&D Program of Yunnan Province (202303AC100025).

Author Contributions

All authors made a significant contribution to the work reported, whether that is in the conception, study design, execution, acquisition of data, analysis and interpretation, or in all these areas; took part in drafting, revising or critically reviewing the article; gave final approval of the version to be published; have agreed on the journal to which the article has been submitted; and agree to be accountable for all aspects of the work.

Funding

This study was supported by the National Natural Science Foundation of China (grant no. 82060723).

Disclosure

The authors report no conflicts of interest in this work.

References

1. Roth GA, Mensah GA, Johnson CO. et al. Global burden of cardiovascular diseases and risk factors, 1990-2019: update from the GBD 2019 study. *J Am Coll Cardiol*. 2020;76(25):2982–3021. doi:10.1016/j.jacc.2020.11.010
2. Hausenloy DJ, Yellon DM. Ischaemic conditioning and reperfusion injury. *Nat Rev Cardiol*. 2016;13(4):193–209. doi:10.1038/nrcardio.2016.5
3. Zhao T, Wu W, Sui L, et al. Reactive oxygen species-based nanomaterials for the treatment of myocardial ischemia reperfusion injuries. *Bioact Mater*. 2022;7:47–72. doi:10.1016/j.bioactmat.2021.06.006
4. Peoples JN, Saraf A, Ghazal N, Pham TT, Kwong JQ. Mitochondrial dysfunction and oxidative stress in heart disease. *Exp Mol Med*. 2019;51(12):1–13. doi:10.1038/s12276-019-0355-7
5. Sinha K, Das J, Pal PB, Sil PC. Oxidative stress: the mitochondria-dependent and mitochondria-independent pathways of apoptosis. *Arch Toxicol*. 2013;87(7):1157–1180. doi:10.1007/s00204-013-1034-4
6. Hu X, Ma R, Lu J, et al. IL-23 promotes myocardial I/R injury by increasing the inflammatory responses and oxidative stress reactions. *Cell Physiol Biochem*. 2016;38(6):2163–2172. doi:10.1159/000445572
7. Sanderson TH, Gallaway M, Kumar R. Unfolding the unfolded protein response: unique insights into brain ischemia. *Int J Mol Sci*. 2015;16(4):7133–7142. doi:10.3390/ijms16047133
8. Chen X, Wang Y, Xie X, et al. Heme oxygenase-1 reduces sepsis-induced endoplasmic reticulum stress and acute lung injury. *Mediators Inflamm*. 2018;2018:9413876. doi:10.1155/2018/9413876
9. Cao SS, Kaufman RJ. Endoplasmic reticulum stress and oxidative stress in cell fate decision and human disease. *Antioxid Redox Signal*. 2014;21(3):396–413. doi:10.1089/ars.2014.5851
10. Xia B, Li Q, Wu J, et al. Sinomenine confers protection against myocardial ischemia reperfusion injury by preventing oxidative stress, cellular apoptosis, and inflammation. *Front Pharmacol*. 2022;13:922484. doi:10.3389/fphar.2022.922484
11. Parham S, Kharazi AZ, Bakhsheshi-Rad HR, et al. Antioxidant, antimicrobial and antiviral properties of herbal materials. *Antioxidants*. 2020;9(12). doi:10.3390/antiox9121309
12. Jiang Z, Cui X, Qu P, Shang C, Xiang M, Wang J. Roles and mechanisms of puerarin on cardiovascular disease:A review. *Biomed Pharmacother*. 2022;147:112655. doi:10.1016/j.biopha.2022.112655
13. Yang Y, Li X, Chen G, et al. Traditional Chinese medicine compound (Tongxinluo) and clinical outcomes of patients with acute myocardial infarction: the CTS-AMI randomized clinical trial. *JAMA*. 2023;330(16):1534–1545. doi:10.1001/jama.2023.19524
14. Zhang JY, Chen QQ, Li J, Zhang L, Qi LW. Neuraminidase 1 and its inhibitors from chinese herbal medicines: an emerging role for cardiovascular diseases. *Am J Chin Med*. 2021;49(4):843–862. doi:10.1142/s0192415x21500403
15. Wei XH, Chen J, Wu XF, et al. Salvianolic acid B alleviated myocardial ischemia-reperfusion injury via modulating SIRT3-mediated crosstalk between mitochondrial ROS and NLRP3. *Phytomedicine*. 2025;136:156260. doi:10.1016/j.phymed.2024.156260
16. Atanasov AG, Zotchev SB, Dirsch VM, Supuran CT. Natural products in drug discovery: advances and opportunities. *Nat Rev Drug Discov*. 2021;20(3):200–216. doi:10.1038/s41573-020-00114-z
17. Yang J, Tian S, Zhao J, Zhang W. Exploring the mechanism of TCM formulae in the treatment of different types of coronary heart disease by network pharmacology and machining learning. *Pharmacol Res*. 2020;159:105034. doi:10.1016/j.phrs.2020.105034
18. Dai J, Qiu L, Lu Y, Li M. Recent advances of traditional Chinese medicine against cardiovascular disease: overview and potential mechanisms. *Front Endocrinol*. 2024;15:1366285. doi:10.3389/fendo.2024.1366285
19. Yu ZP, Mu YS, Zhao ZX, Wang FC. Antiarrhythmic effects of crebanine. *Zhongguo Zhong Yao Za Zhi*. 1992;17(11):685–7,704.
20. Lam KY, Ku CF, Wang HY, et al. Authentication of Acori Tatarinowii Rhizoma (Shi Chang Pu) and its adulterants by morphological distinction, chemical composition and ITS sequencing. *Chin Med*. 2016;11:41. doi:10.1186/s13020-016-0113-x
21. Feng P, Chen Y, Sun K, et al. Volatile oil from Acori graminei Rhizoma affected the synaptic plasticity of rats with tic disorders by modulating dopaminergic and glutamatergic systems. *J Ethnopharmacol*. 2024;335:118676. doi:10.1016/j.jep.2024.118676
22. Park C, Cha HJ, Hwangbo H, et al. β-asarone alleviates high-glucose-induced oxidative damage via inhibition of ROS generation and inactivation of the NF-κB/NLRP3 inflammasome pathway in human retinal pigment epithelial cells. *Antioxidants*. 2023;12(7):1410. doi:10.3390/antiox12071410
23. Zhong RN, Wang XH, Wan L, et al. Study on preparation of volatile oil from Acorus tatarinowii self-nanoemulsion dropping pills and its protective effect on acute myocardial ischemia injury. *Zhongguo Zhong Yao Za Zhi*. 2019;44(7):1357–1362. doi:10.19540/j.cnki.cjcmm.20181220.006
24. Xiao B, Huang X, Wang Q, Wu Y. Beta-asarone alleviates myocardial ischemia-reperfusion injury by inhibiting inflammatory response and NLRP3 inflammasome mediated pyroptosis. *Biol Pharm Bull*. 2020;43(7):1046–1051. doi:10.1248/bpb.b19-00926
25. Xiang M, Lu Y, Xin L, et al. Role of oxidative stress in reperfusion following myocardial ischemia and its treatments. *Oxid Med Cell Longev*. 2021;2021:6614009. doi:10.1155/2021/6614009
26. Zeng J, Jin Q, Ruan Y, et al. Inhibition of TGFβ-activated protein kinase 1 ameliorates myocardial ischaemia/reperfusion injury via endoplasmic reticulum stress suppression. *J Cell Mol Med*. 2020;24(12):6846–6859. doi:10.1111/jcmm.15340
27. Mariángelo JIE, Román B, Silvestri MA, et al. Chemical chaperones improve the functional recovery of stunned myocardium by attenuating the endoplasmic reticulum stress. *Acta Physiol*. 2020;228(2):e13358. doi:10.1111/apha.13358
28. Cimellaro A, Perticone M, Fiorentino TV, Sciacqua A, Hribal ML. Role of endoplasmic reticulum stress in endothelial dysfunction. *Nutr, Metab Cardiovasc Dis*. 2016;26(10):863–871. doi:10.1016/j.numecd.2016.05.008
29. Lee WS, Yoo WH, Chae HJ. ER stress and autophagy. *Curr Mol Med*. 2015;15(8):735–745. doi:10.2174/1566524015666150921105453

30. Chen YH, Lin H, Wang Q, Hou JW, Mao ZJ, Li YG. Protective role of silibinin against myocardial ischemia/reperfusion injury-induced cardiac dysfunction. *Int J Biol Sci*. 2020;16(11):1972–1988. doi:10.7150/ijbs.39259
31. Zhang J, Wang L, Xie W, et al. Melatonin attenuates ER stress and mitochondrial damage in septic cardiomyopathy: a new mechanism involving BAP31 upregulation and MAPK-ERK pathway. *J Cell Physiol*. 2020;235(3):2847–2856. doi:10.1002/jcp.29190
32. Oyadomari S, Koizumi A, Takeda K, et al. Targeted disruption of the Chop gene delays endoplasmic reticulum stress-mediated diabetes. *J Clin Invest*. 2002;109(4):525–532. doi:10.1172/jci14550
33. Zhao ZQ. Oxidative stress-elicited myocardial apoptosis during reperfusion. *Curr Opin Pharmacol*. 2004;4(2):159–165. doi:10.1016/j.coph.2003.10.010
34. Kalogeris T, Bao Y, Korthuis RJ. Mitochondrial reactive oxygen species: a double edged sword in ischemia/reperfusion vs preconditioning. *Redox Biol*. 2014;2:702–714. doi:10.1016/j.redox.2014.05.006
35. Li L, Zhou Y, Li Y, et al. Aqueous extract of Cortex Dictamni protects H9c2 cardiomyocytes from hypoxia/reoxygenation-induced oxidative stress and apoptosis by PI3K/Akt signaling pathway. *Biomed Pharmacother*. 2017;89:233–244. doi:10.1016/j.biopha.2017.02.013
36. Haunstetter A, Izumo S. Apoptosis: basic mechanisms and implications for cardiovascular disease. *Circ Res*. 1998;82(11):1111–1129. doi:10.1161/01.res.82.11.1111
37. Yang G, Min D, Yan J, Yang M, Lin G. Protective role and mechanism of snakegourd peel against myocardial infarction in rats. *Phytomedicine*. 2018;42:18–24. doi:10.1016/j.phymed.2018.03.014
38. Liu XM, Chen QH, Hu Q, et al. Dexmedetomidine protects intestinal ischemia-reperfusion injury via inhibiting p38 MAPK cascades. *Exp Mol Pathol*. 2020;115:104444. doi:10.1016/j.yexmp.2020.104444
39. Ma L, Liu H, Xie Z, et al. Ginsenoside Rb3 protects cardiomyocytes against ischemia-reperfusion injury via the inhibition of JNK-mediated NF-κB pathway: a mouse cardiomyocyte model. *PLoS One*. 2014;9(8):e103628. doi:10.1371/journal.pone.0103628
40. Tian H, Zhao X, Zhang Y, Xia Z. Abnormalities of glucose and lipid metabolism in myocardial ischemia-reperfusion injury. *Biomed Pharmacother*. 2023;163:114827. doi:10.1016/j.biopha.2023.114827
41. MacLean A, Legendre F, Appanna VD. The tricarboxylic acid (TCA) cycle: a malleable metabolic network to counter cellular stress. *Crit Rev Biochem Mol Biol*. 2023;58(1):81–97. doi:10.1080/10409238.2023.2201945
42. Lai Q, Yuan GY, Wang H, et al. Exploring the protective effects of schizandrol A in acute myocardial ischemia mice by comprehensive metabolomics profiling integrated with molecular mechanism studies. *Acta Pharmacol Sin*. 2020;41(8):1058–1072. doi:10.1038/s41401-020-0377-7
43. Tang Q, Tan P, Ma N, Ma X. Physiological functions of threonine in animals: beyond nutrition metabolism. *Nutrients*. 2021;13(8):2592. doi:10.3390/nu13082592
44. Liu YT, Jia HM, Chang X, Ding G, Zhang HW, Zou ZM. The metabolic disturbances of isoproterenol induced myocardial infarction in rats based on a tissue targeted metabonomics. *Mol Biosyst*. 2013;9(11):2823–2834. doi:10.1039/c3mb70222g
45. Løfgren B, Povlsen JA, Rasmussen LE, et al. Amino acid transamination is crucial for ischaemic cardioprotection in normal and preconditioned isolated rat hearts--focus on L-glutamate. *Exp Physiol*. 2010;95(1):140–152. doi:10.1113/expphysiol.2009.049452
46. King N, McGivan JD, Griffiths EJ, Halestrap AP, Suleiman MS. Glutamate loading protects freshly isolated and perfused adult cardiomyocytes against intracellular ROS generation. *J Mol Cell Cardiol*. 2003;35(8):975–984. doi:10.1016/s0022-2828(03)00182-2
47. Williams H, King N, Griffiths EJ, Suleiman MS. Glutamate-loading stimulates metabolic flux and improves cell recovery following chemical hypoxia in isolated cardiomyocytes. *J Mol Cell Cardiol*. 2001;33(12):2109–2119. doi:10.1006/jmcc.2000.1474
48. Kristiansen SB, Løfgren B, Støttrup NB, et al. Cardioprotection by L-glutamate during postischaemic reperfusion: reduced infarct size and enhanced glycogen resynthesis in a rat insulin-free heart model. *Clin Exp Pharmacol Physiol*. 2008;35(8):884–888. doi:10.1111/j.1440-1681.2008.04914.x
49. Jefferies H, Coster J, Khalil A, Bot J, McCauley RD, Hall JC. Glutathione. *ANZ J Surg*. 2003;73(7):517–522. doi:10.1046/j.1445-1433.2003.02682.x
50. Magi S, Piccirillo S, Amoroso S, Lariccia V. Excitatory Amino Acid Transporters (EAATs): glutamate transport and beyond. *Int J Mol Sci*. 2019;20(22):5674. doi:10.3390/ijms20225674
51. Steffen BT, Duprez D, Szklo M, Guan W, Tsai MY. Circulating oleic acid levels are related to greater risks of cardiovascular events and all-cause mortality: the multi-ethnic study of atherosclerosis. *J Clin Lipidol*. 2018;12(6):1404–1412. doi:10.1016/j.jacl.2018.08.004
52. Zou LH, Liu JP. The myocardial metabolic profiling of extracorporeal circulation based on gas chromatography-mass spectrometry in a rabbit model. *Chin J Extracorporeal Circ*. 2021;04(19):228–234.
53. Malinowsky K, Nitsche U, Janssen KP, et al. Activation of the PI3K/AKT pathway correlates with prognosis in stage II colon cancer. *Br J Cancer*. 2014;110(8):2081–2089. doi:10.1038/bjc.2014.100
54. Jin ES, Lee MH, Malloy CR. (13) C NMR of glutamate for monitoring the pentose phosphate pathway in myocardium. *NMR Biomed*. 2021;34(7):e4533. doi:10.1002/nbm.4533
55. Scantlebery AM, Tammaro A, Mills JD, et al. The dysregulation of metabolic pathways and induction of the pentose phosphate pathway in renal ischaemia-reperfusion injury. *J Pathol*. 2021;253(4):404–414. doi:10.1002/path.5605
56. Cadenas S. ROS and redox signaling in myocardial ischemia-reperfusion injury and cardioprotection. *Free Radic Biol Med*. 2018;117:76–89. doi:10.1016/j.freeradbiomed.2018.01.024
57. Werns SW, Shea MJ, Lucchesi BR. Free radicals and myocardial injury: pharmacologic implications. *Circulation*. 1986;74(1):1–5. doi:10.1161/01.cir.74.1.1
58. Kurian GA, Rajagopal R, Vedantham S, Rajesh M. The role of oxidative stress in myocardial ischemia and reperfusion injury and remodeling: revisited. *Oxid Med Cell Longev*. 2016;2016:1656450. doi:10.1155/2016/1656450
59. Moens AL, Claeys MJ, Timmermans JP, Vrints CJ. Myocardial ischemia/reperfusion-injury, a clinical view on a complex pathophysiological process. *Int J Cardiol*. 2005;100(2):179–190. doi:10.1016/j.ijcard.2004.04.013
60. Murphy E, Steenbergen C. Estrogen regulation of protein expression and signaling pathways in the heart. *Biol Sex Differ*. 2014;5(1):6. doi:10.1186/2042-6410-5-6
61. Li D, Wang X, Huang Q, Li S, Zhou Y, Li Z. Cardioprotection of CAPE-oNO(2) against myocardial ischemia/reperfusion induced ROS generation via regulating the SIRT1/eNOS/NF-κB pathway in vivo and in vitro. *Redox Biol*. 2018;15:62–73. doi:10.1016/j.redox.2017.11.023